Exp. Theo. NANOTECHNOLOGY 10 (2026) 769-779 https://doi.org/10.56053/10.2.769

Utilization of multitemporal satellite imagery and forest canopy density (FCD) model for analyzing changes in forest density in Mosul province, Iraq

Inbethaq Mohammed Ali Abdulameer [*], *Ali Adnan N. Al-Jasim, Nehad Hameed*

Department of physics, College of Education for Pure Science (Ibn Al-Haitham), University of Baghdad, Iraq
[*]) Email: Inbethaq.m@ihcoedu.uobaghdad.edu.iq

Received 15/1/2026, *Received in revised form* 2/3/2026, *Accepted* 17/3/2026, *Published* 15/4/2026

Forest cover in Mosul Province experienced significant changes following the 2014 occupation. These changes can be effectively analyzed using multitemporal remote sensing imagery. This study aims to evaluate the ability of multi-temporal Landsat 8 images and the Forest Canopy Density (FCD) model to detect changes in forest canopy density in a protected forest in Mosul Governorate during the period from 2014 to 2025. The remote sensing data used in this research are Landsat 8 images captured on March 21, 2014, and April 4, 2025. The method employed is FCD modeling, which produces pixel-level canopy density estimates. The results of the FCD model are then used to analyze changes in canopy density following the occupation. The findings of this study show that Landsat 8 imagery can be effectively used to detect canopy density in the Mosul Province protected forest, with accuracies of 82.65% before the occupation and 80.71% after. There are significant changes in canopy density post-occupation: approximately 598.17 acres of forest experienced a decrease in canopy density, 168.05 acres remained unchanged, and 133.78 acres showed an increase in canopy density.

Keywords: Landsat 8; FCD modeling; Canopy density changes; Advanced vegetation.

1. INTRODUCTION

Remote sensing offers a significant advantage in terms of temporal resolution. The difference in image acquisition times (temporal resolution) enables the monitoring of phenomena or objects on the Earth's surface that change over a specific period. Objects captured at different times may show variations in spectral reflectance; for example, the spectral reflectance of vegetation can be influenced by the current season. Vegetation, as one of the objects that can be identified in satellite imagery, has a distinctive spectral reflectance, particularly in the infrared band. This makes the infrared band especially suitable for studying vegetation, including dense groups of vegetation that form forests. Landsat 8 is equipped with 11 spectral bands, with Band 5 being the near-infrared band, which is particularly useful for identifying vegetation [1]. As a result, numerous remote sensing studies have been conducted in the field of vegetation, including research focused specifically on forests. The advantage of remote sensing in capturing multitemporal data, combined with the distinctive reflectance characteristics of vegetation in the infrared band, enables the analysis of forest canopy density changes [2] such as those observed in the protected forest area of Mosul Province. One effective model for analyzing forest canopy density is the Forest Canopy Density (FCD) model. A key strength of the FCD model is that it does not rely solely on vegetation indicators [3]; it also considers other factors negatively correlated with vegetation, such as surface temperature and bare soil, as well as shadow [4], which also has a negative correlation with vegetation [5]. Another advantage of the FCD model is its ability to assess the structural composition of forest areas. The forest canopy density is evaluated based on percentage values generated through the FCD model. This makes FCD a highly suitable method for analyzing changes in forest canopy density following a violent occupation. The pixel-based percentage values for the four main components of the FCD model are derived from the Advanced Vegetation Index (AVI), Bare Soil Index (BI), Shadow Index (SI), and Thermal Index (TI) [3]. This study aims to evaluate the effectiveness of multitemporal Landsat 8 imagery and the Forest Canopy Density (FCD) model in detecting changes in canopy density within the Mosul Province Protected Forest area in 2014 and 2025. Recent advances in nanomaterials, including quantum dots, carbon nanotubes, and graphene-based composites, have enabled the fabrication of highly sensitive detectors and lightweight optical components that boast superior spectral and spatial resolution. These nanostructured materials enhance sensor responsiveness to specific wavelengths, especially those in the infrared and thermal bands [6], which are essential in vegetation and canopy studies. The FCD model is first proposed by Rikimaru et al. [7] since gained extensive use in forest ecology and land-cover change detection. It is successfully applied in showing the changes in canopy density due to different disturbance conditions in research. Integrating multiple indices, such as AVI, BI, SI, and TI, provides comprehensive insight into forest health and structure. These studies [3,4], suggest that approaches based on FCD prove better than traditional vegetation indices in distinguishing between degraded and dense forest classes, especially under post-disturbance analysis.

2. RESEARCH METHODS

This study is conducted in the Hadba Model Forest in Mosul Province, which is administratively located on the eastern bank of the Tigris River, on the northern side of the city. The northern part of Mosul Province sits at an Altitude of 223 meters above sea level.The Mosul Province forest lies within the coordinates of 36°21′0″- N Latitude and 43°09′0″E.Longitude covers an area of approximately 900 acres, and most of the forest trees are Eucalyptus trees, Pinus trees and Cypress [8]. The most recent occupation occurred in June 2014, causing significant forest damage in the surrounding area.

To assess canopy density, this study utilized Landsat 8 satellite imagery captured on March 21, 2014, and April 4, 2025. These two dates represent the forest conditions in 2014 and 2025, respectively. Landsat 8, launched on February 11, 2013, is equipped with 11 spectral bands, including: Coastal

(0.43–0.45 μm), Blue (0.45–0.51 μm), Green (0.53–0.59 μm), Red (0.64–0.67 μm), Near-Infrared (NIR) (0.85–0.88 μm), Short-Wave Infrared 1 (SWIR 1) (1.57–1.65 μm), Short-Wave Infrared 2 (SWIR 2) (2.11–2.29 μm), Panchromatic (0.50–0.68 μm), Cirrus (1.36–1.38 μm), Thermal Infrared 1 (TIRS 1) (10.6–11.9 μm), Thermal Infrared 2 (TIRS 2) (11.5–12.51 μm) [9].

In addition to satellite imagery, this research also made use of Iraq's Topographic Base Map for geometric correction and to define the administrative boundaries of the study area. Before modelling the canopy density, the Landsat 8 images underwent preprocessing, including both geometric and radiometric corrections.

- Geometric correction is performed using the image-to-map method, where the RBI map served as the reference to align the imagery.
- Radiometric correction aimed to normalize the image bands. This process is carried out in two stages, beginning with the conversion of digital number (DN) values into reflectance values.

The digital number (DN) values from the Landsat imagery are first converted into radiance and then into reflectance values. Topographic correction is also applied to account for terrain effects. Specifically for Band 10 (thermal infrared), the radiometric correction process continued until surface temperature values are obtained. For the other bands, the correction process is carried out until surface reflectance values are derived [10].

Forest Canopy Density (FCD) is a method used to estimate forest canopy cover by incorporating factors such as vegetation, bare soil, temperature, and shadow. The FCD model is commonly used in forest mapping and monitoring, where canopy density serves as a key parameter representing forest conditions. The FCD model uses several indices, including the Advanced Vegetation Index (AVI), Bare Soil Index (BI), Shadow Index (SI or Scaled Shadow Index/SSI), and Thermal Index (TI) [3].

These indices are calculated using the following Landsat 8 bands:Band 2 (Blue), Band 3 (Green), Band 4 (Red), Band 5 (Near-Infrared/NIR), Band 6 (Short-Wave Infrared 1/SWIR 1), Band 7 (Short-Wave Infrared 2/SWIR 2), Band 10 (Thermal Infrared).

1. Advanced vegetation index (AVI)

AVI is used to assess chlorophyll content and the overall greenness of vegetation. It highlights dense vegetation by combining reflectance from the red and near-infrared bands. The formula used is [11]:

$$AVI = ((Band5 + 1) \times (256 - Band4) \times (Band5 - Band4))\text{^}(1/3) \quad (1)$$

2. Bare soil index (BI)

BI emphasizes the presence of bare soil and distinguishes it from vegetation and other land cover types. It utilizes reflectance from the SWIR, NIR, red, and blue bands. The formula is [11]:

$$BI = (((Band6 + Band4) - (Band5 + Band2)) / ((Band6 + Band4) + (Band5 + Band2))) \times 100 + 100 \quad (2)$$

3. Shadow index (SI)

SI is used to identify and assess shadow areas in the imagery, especially shadows cast by vegetation. It uses reflectance from the blue, green, and red bands, and the formula is [11]:

$$SI = ((256 - Band2) \times (256 - Band3) \times (256 - Band4))^{1/3} \quad (3)$$

4. Thermal index (TI)

TI is based on two main factors that influence how cool a forested area appears [12]::

- The shielding effect of the canopy, which blocks and absorbs solar energy.
- The evaporative cooling effect from leaf surfaces, which reduces surface temperature.

Temperature data from the thermal infrared band is used to help distinguish between bare soil and non-vegetated shadow areas.

To obtain surface temperature values, the digital number from the thermal band is first converted to radiance. Then, brightness temperature is calculated using Band 10. The following formula is used to convert radiance to temperature:

$$T = K_2 / \ln(K_1 / L\lambda + 1) \quad (4)$$

Where: T = brightness temperature (Kelvin), K1 & K2= thermal conversion constant at band 10, Lλ = radiance value of the thermal band.

There is a correlation between vegetation and forest shadow parameters. As vegetation increases, the amount of shadow also increases. Therefore, when forest density becomes higher, the shadows beneath the canopy also increase, which in turn leads to a rise in the Shadow Index (SI) value. The Thermal Index (TI), on the other hand, increases when vegetation decreases. This is because more exposed or open ground (indicating a lack of vegetation cover) tends to have higher surface temperatures. the combination of the four indices used in the Forest Canopy Density (FCD) model—AVI, BI, SI, and TI—produces a correlated relationship among all of them [7].

The characteristics of the combination of four indices used in the Forest Canopy Density (FCD) model. Based on Table 1, when the Advanced Vegetation Index (AVI) is high, the FCD value is also likely to be high, whereas a low AVI value indicates an object that is likely open land. A high Bare Soil Index (BI) value indicates open land, whereas a low BI value most likely corresponds to vegetation. The Shadow Index (SI), however, decreases as FCD decreases and tends to have low values for objects such as shrubs and open land. The Thermal Index (TI) behaves in the opposite way to SI. TI values increase as vegetation decreases, showing high values for open land and low values for areas with high FCD.

Table 1. Characteristics of the Combination among Four Indices [12].

Index	High FCD	Low FCD	Shrub	Bare Land
Advanced Vegetation Index (AVI)	High	Moderate	High	Low
Bare Soil Index (BI)	Low	Low	Low	High
Shadow Index (SI)	High	Moderate	Low	Low
Temperature Index (TI)	Low	Moderate	Moderate	High

Vegetation Density (VD) is derived as a synthesis of AVI and BI. Vegetation density here refers to the cover or proportion of vegetation present. The vegetation density (VD) refers to the proportion of ground surface covered by the projection of plant canopies. This method uses Principal Component Analysis (PCA) because AVI and BI are negatively correlated [13].

The Scaled Shadow Index (SSI) is derived from the histogram of the Shadow Index (SI) adjusted by the Thermal Index (TI) to differentiate between forest and ground vegetation based on shadow and

surface temperature. Areas with an SSI value of zero indicate forests with the lowest shadow values, while areas with an SSI value of 100 indicate forests with the highest shadow values. By developing SSI, it becomes possible to distinguish between canopy vegetation and vegetation on the ground [7] The integration of VD and SSI produces the forest canopy density (FCD) value. The canopy density index is calculated using the equation [7]:

$$FCD= (VDxSSI+1)1/2-1 \quad (5)$$

This integrated model generates canopy density data for each pixel. The FCD percentage ranges from 0% to 100%, where 0% represents the absence of canopy cover and indicates an area dominated by open land. As the FCD percentage increases, a larger pixel area is covered by the canopy. additionally, distinct strata develop, and heterogeneity increases, preventing sunlight from reaching the forest floor. The canopy density modeling for Mosul Province Forest before and after the occupation is accuracy-tested using the Standard Error of Estimation (SEE) method. SEE evaluates the accuracy by considering the difference between modeled canopy density and actual field measurements. Field measurements to obtain actual canopy density are conducted in March 2025 with 41 sample points. The accuracy-tested FCD model results are then used to analyze canopy density changes after the 2014 occupation [13].

The canopy density maps modeled using FCD for 2014 (pre-occupation) and 2025 (post-occupation) are used to detect changes in canopy density using the Combine method in ArcGIS 10.2. This method produces information about changes in density in both tabular and map form. Combine is a raster overlay technique that analyzes changes in pixels located at the same geographic positions but from two different time periods (or cells) and assigns a new identity based on the detected changes. Based on the FCD models for 2014 and 2025, overlay analysis is conducted to determine the area extent experiencing change and to analyze changes in canopy density [14].

3. RESULTS AND DISCUSSION

The Advanced Vegetation Index (AVI), Bare Soil Index (BI), Shadow Index or Scaled Shadow Index (SSI), and Thermal Index (TI) are processed using FCD Mapper software to produce forest canopy density (FCD) expressed as a percentage (%). The calculations of AVI and BI using topographically corrected Landsat images also yielded vegetation density (VD) values, also expressed in percentage. The VD results for Landsat 8 images acquired on March 21, 2014, and April 4, 2025. Figure 1 illustrates that vegetation density is low near the northern part on March 21, 2014, while the areas surrounding it had vegetation densities ranging from 60% to 100%, with some patches showing densities between 40% and 50%. In contrast, the vegetation density after the occupation (Landsat 8 image from April 4, 2025) showed that the area around the northern part is dominated by very low vegetation density, between 0% and 10%. This clearly indicates the impact of the 2014 occupation on vegetation at Mosul Province, where vegetation density drastically decreased. The most dominant vegetation density class in the April 4, 2025 image is 0–10%, whereas in the March 21, 2014 image it is 60–70% [15-20].

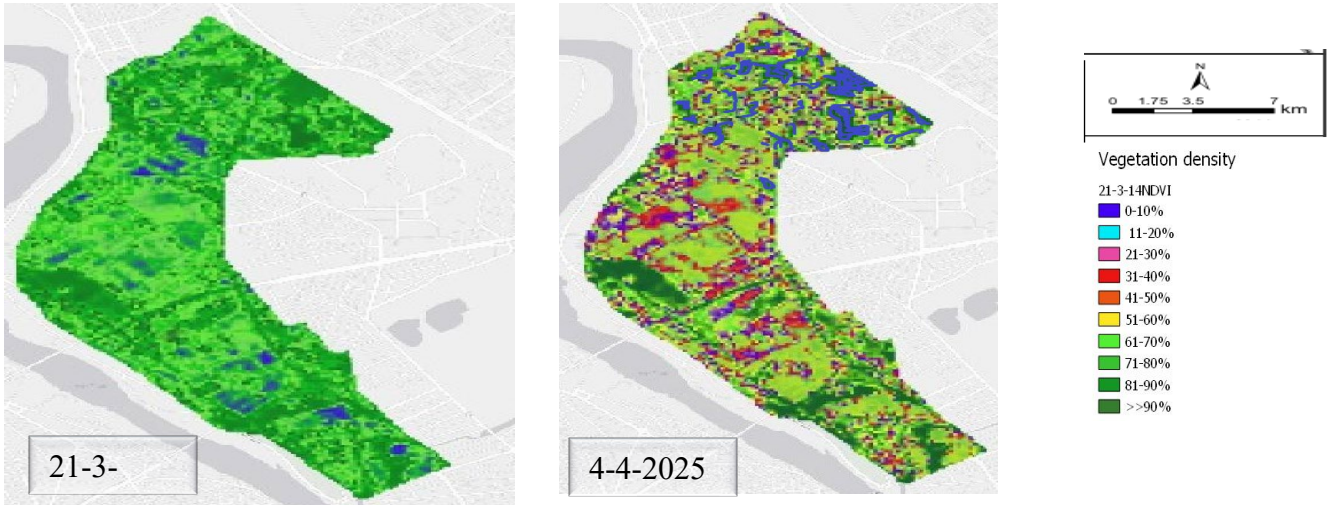

Figure 1 Vegetation density of Landsat 8 imagery.

The SSI results for the Landsat 8 images from March 21, 2014, and April 4, 2025, are shown in Figure 2. As seen in Figure 2, the SSI values in the March 21, 2014, Landsat 8 image are mostly in the range of 70–100%, which is visually represented by dominant green colors. SSI values greater than 90% appear on the forested slopes, indicating low temperatures and high shadow levels—conditions typical of areas with dense vegetation. This indirectly confirms that Mosul Forests is densely vegetated, with relatively low temperatures and high canopy shadows [21].

The Landsat 8 image from April 4, 2025, shows SSI values mostly in the 80–100% range but also reveals a significant increase in the area with SSI values between 0–10% around the northern part compared to the March 21, 2014 image. Low SSI values indicate high thermal index values and low shadow index values. This aligns with the condition of the northern part area affected by the occupation, where vegetation is reduced or lost, exposing open land with relatively high temperatures and minimal shading. Based on this, it can be concluded that the SSI results from the April 4, 2025, Landsat 8 image accurately reflect the post-occupation conditions of 2014 [22].

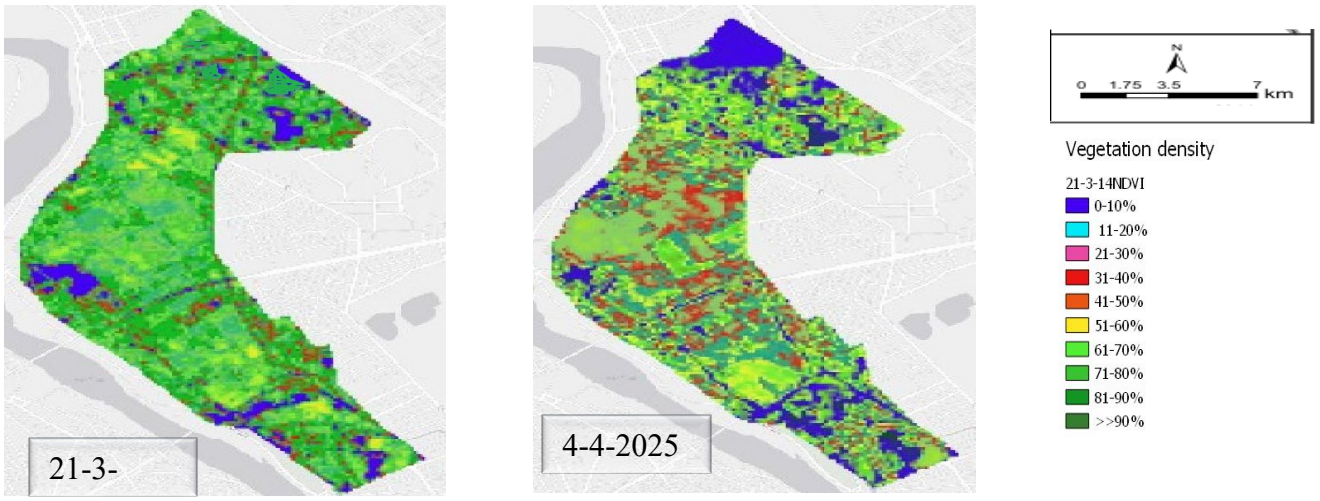

Figure 2 Scaled shadow index of Landsat 8 image.

VD and SSI are then processed to produce an estimated Forest Canopy Density (FCD) ranging from 0 to 100, assumed to represent the percentage per pixel. The FCD maps for 2014 and 2025 are reclassified into 10 classes to simplify the detection of changes in canopy density [23]. The FCD results for the Landsat 8 images from March 21, 2014, and April 4, 2025, can be seen in Figures 3 and 4.

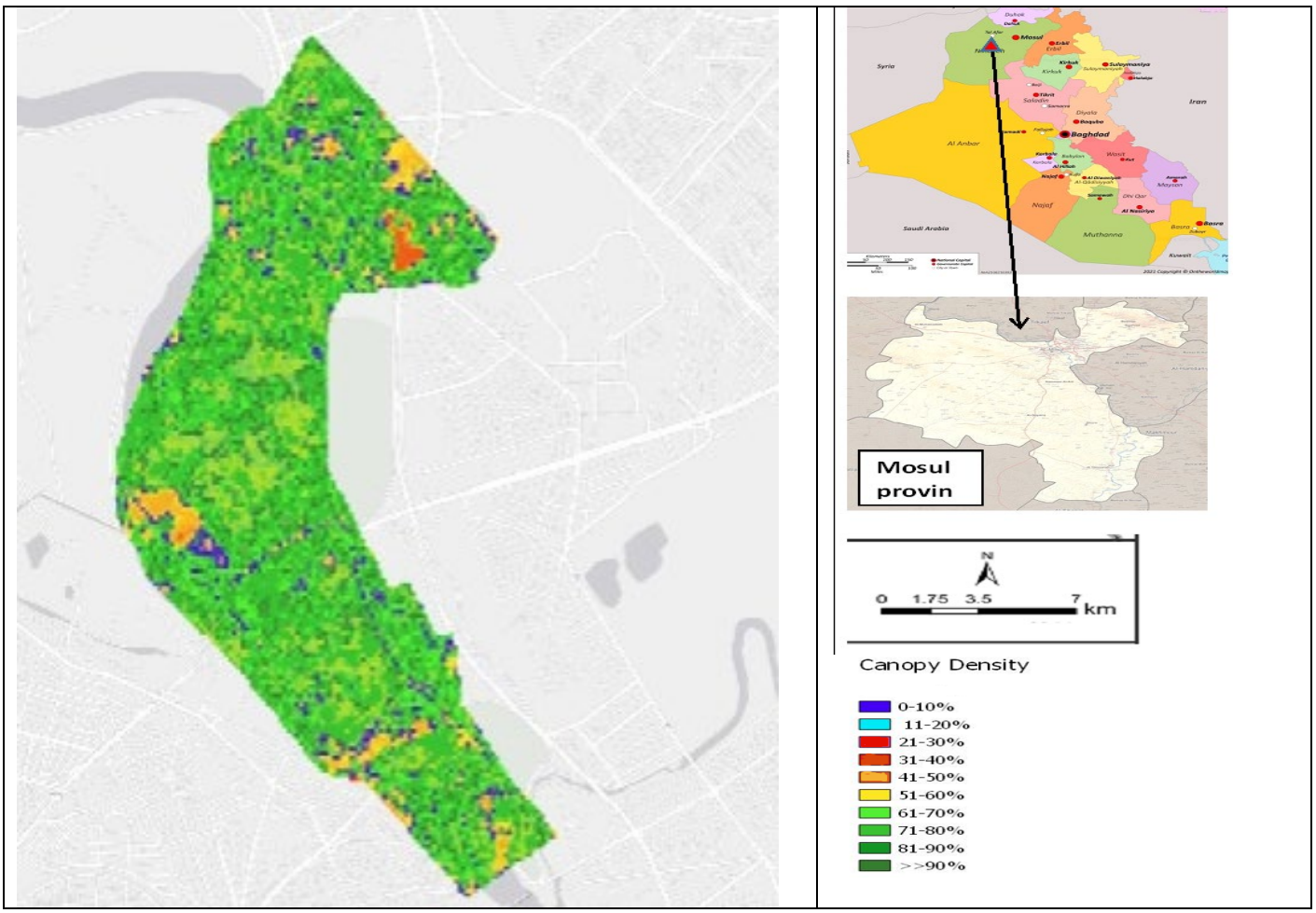

Figure 3 Map of Mosul Forest canopy density on March 21, 2014.

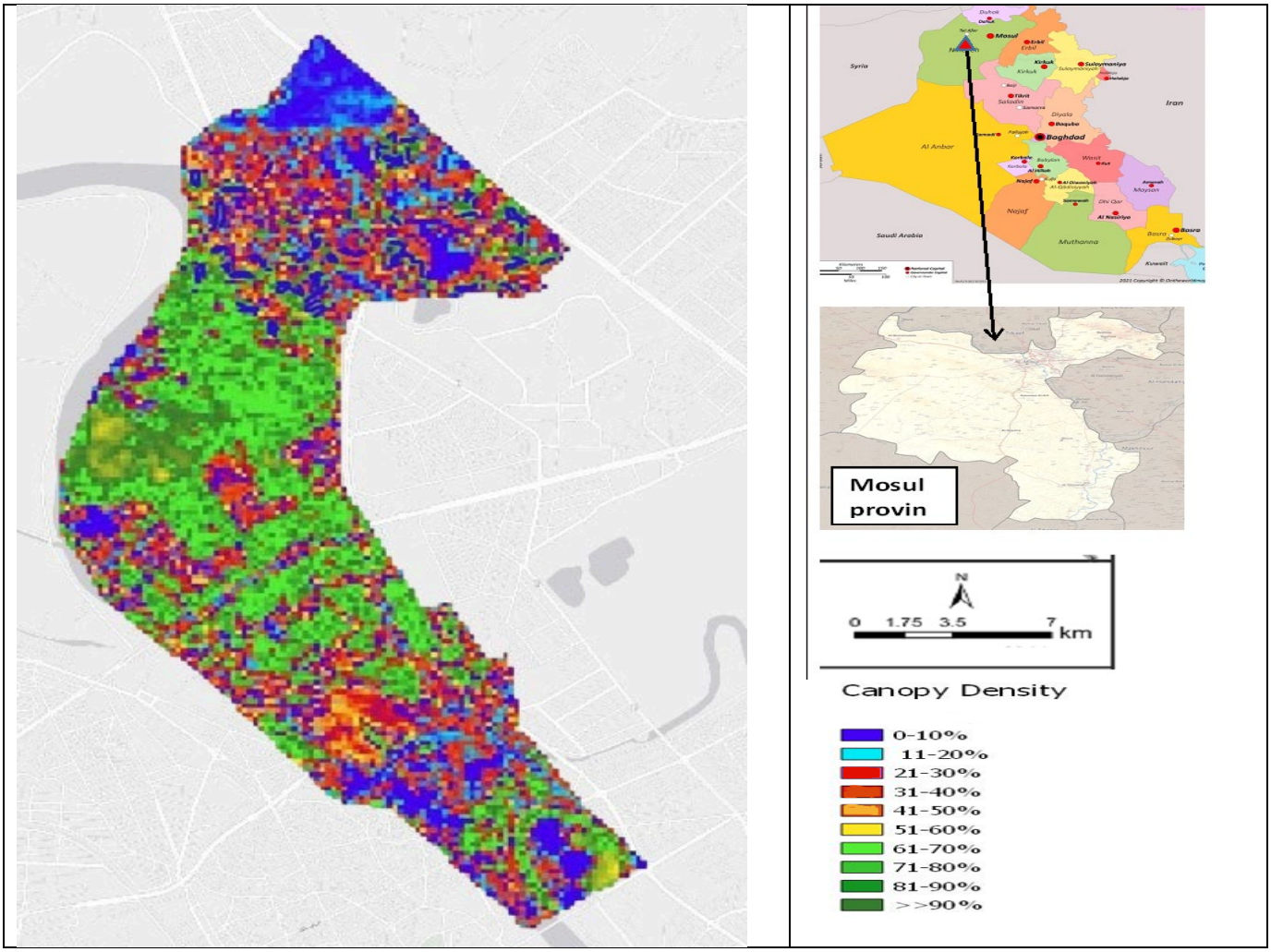

Figure 4 Map of Mosul Forest canopy density on April 4, 2025.

The canopy density maps use color symbols based on the FCD Mapper output, including blue, cyan, magenta, red, orange, yellow, and a gradient from light green to dark green. The canopy density appearance in Figure 3 is mainly dominated by the 72–80% density class.

Covering an area of 317.64 acres, this density class represents forest conditions where the canopy covers 71–80% of each pixel area. In this class, distinct canopy strata are clearly visible, and species heterogeneity increases. it can be seen that the density class with the fewest pixels is the >90% canopy density class, covering only 13 acres. The area and pixel count for each canopy density class in Al Mosul Province's Forest before the occupation are shown in Table 2. When visually observed on the map, the dominant colors are shades of green, representing canopy densities between 51% and 90%. The most noticeable feature is the presence of canopy density The red-colored area (21–30%) appears as an extended region, representing a zone of varying vegetation density within the forest.

The Canopy Density Map of Mosul Province after the 2014 occupation shows a much larger area with canopy density between 1–10%. This 1–10% canopy density class is located in the central north area of the forest and along barren roads spreading in various directions. The total area for this canopy density class is 194.61 acres. The canopy density classes after the occupation, based on area and pixel count, are presented in Table 3. Another fairly dominant canopy density class is 61–70%, covering an

area of 156.20 acres. Observing Figure 3, the 21–30% canopy density class can be seen spreading from the north regime outward in various directions. This class covers an area of 72.20 acres and is shown in magenta.

Table 2 Number of Pixels and Area per Canopy Density Class in 2014.

Canopy Density (%)	Number of Pixels	Area (Ca)
1 – 10	116	25.58
11 – 20	27	6.02
21 – 30	135	30.06
31 – 40	207	45.96
41 – 50	263	58.45
51 – 60	494	109.78
61 – 70	1062	236.16
71 – 80	1428	317.64
81 – 90	313	64.58
>90	13	3.23

Table 3 Number of Pixels and Area per Canopy Density Class in 2025.

Canopy Density (%)	Number of Pixels	Area (Ca)
1 – 10	875	194.61
11 – 20	168	37.37
21 – 30	325	72.20
31 – 40	429	95.47
41 – 50	304	67.64
51 – 60	551	122.61
61 – 70	702	156.20
71 – 80	496	110.38
81 – 90	195	43.46
>90	4	0.89

Accuracy testing for FCD maps of 2014 and 2025 resulted in accuracy values of 82.65% and 80.71%, respectively. These indicate a good level of accuracy, allowing further analysis of changes in canopy density. The Canopy Density Change Map the forest of Mosul Province after the 2014 occupation provides information on canopy density changes per pixel. The forest area experiencing a decrease in canopy density covers 598.17 acres, while the area with unchanged canopy density is 168.05 acres, and the area with increased canopy density is 133.78 acres. The canopy density changes in Figure 5. The map is shown with contrasting colors for clarity: decreasing canopy density is marked in red, unchanged density in yellow and increasing density in green. According to the Canopy Density Change Map after the 2014 occupation, the most dominant change is a decrease in canopy density (red). The occupation caused a significant reduction in canopy density across much of Mosul Province's Forest, with decreases spread throughout the nearby region districts. Areas with stable or increased canopy density are also present but cover much smaller areas compared to those with decreased canopy density.

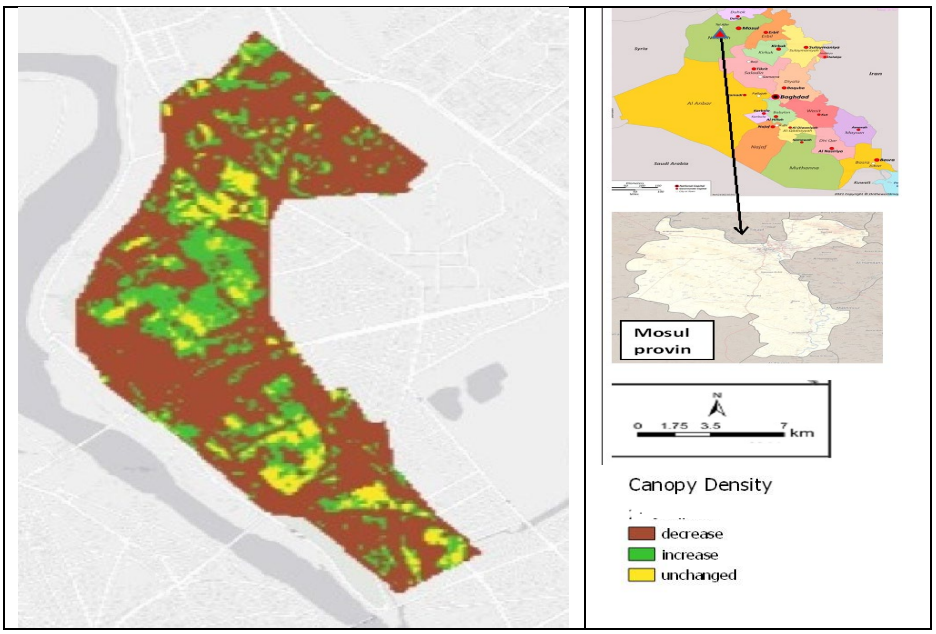

Figure 5 Map of Mosul Forest canopy density before the 2014 occupation.

4. CONCLUSIONS

The accuracy test of the Forest Canopy Density (FCD) map showed the strength of the FCD model for both study periods with a total accuracy of 82.65% for the FCD map of 2014 and 80.71% for the FCD map of 2025, validating the strength of the remote sensing methods and models used. These findings indicate substantial differences in forest canopy density after the occupation phase, signifying major spatiotemporal variations in the forest state. A major reduction in canopy density was noticed for 598.17 acres, largely spread in the northern area and nearby districts, signifying major human interference. Areas with unchanged canopy density were numbered for 168.05 acres, signifying major areas of resilience, whereas areas with 133.78 acres showed an increase in canopy density, likely due to natural regrowth or conservation efforts at the local levels. These observations collectively indicate the efficiency of FCD models in identifying forest degradation and recovery trends and indicate the importance of sustainable forest management practices for effective forest conservation.

References

[1] A.A. Salman, F.K. Mashee, A. Ramahi, I.M. Abdulameer, D.H.M., Exp. Theor. Nanotechnol. 9 (2025) 123 https://doi.org/10.56053/9.1.123
[2] J.H. Azzawi, I.M.A. Abdulameer, AIP Conf. Proc. 2437 (2022) 0670 https://doi.org/10.1063/5.0092338
[3] M.N. Rahman, A. Al Imran, M.S. Sheikh, Heliyon (2024) https://doi.org/10.2139/ssrn.4686244
[4] S. Das, A.K. Das, S. Mishra, Environ. Sci. Eur. 37 (2025) 367 https://doi.org/10.1186/s12302-025-01208-4
[5] K. Kalinaki, B. Sami, I. Gitas, D. Hadjimitsis, Comput. Geosci. 176 (2023) 104949 https://doi.org/10.1016/j.cageo.2023.104949
[6] Y. Zhang, J. Jiang, Z. Zhang, H. Yu, Y. Lian, C. Han, X. Liu, J. Han, H. Zhou, X. Dong, J. Gou, Z. Wu, J. Wang, J. Mater. Chem. C 12 (2024) 16714 https://doi.org/10.1039/D4TC03075A
[7] A. I. A. Ali, M. RASHEED, Experimental and Theoretical NANOTECHNOLOGY, 10 (2026) 239 https://doi.org/10.56053/10.s.239

[8] Z. S. Ahmed, M. RASHEED, H. S. Ahmed, Experimental and Theoretical NANOTECHNOLOGY, 10 (2026) 343 https://doi.org/10.56053/10.s.343
[9] H.N. Abbas, I.M. Abdulameer, AIP Conf. Proc. 2307 (2020) 777 https://doi.org/10.1063/5.0027565
[10] W.T. Andini, N. Nurlina, R. Ichsan, Ecol. Eng. Environ. Technol. 25 (2024) 369 https://doi.org/10.12912/27197050/188498
[11] P. Danoedoro, P. Widayani, I.N. Hidayati, S. Arjasakusuma, D.D. Gupita, H.N. Salsabila, Geocarto Int. 38 (2023) 1 https://doi.org/10.1080/10106049.2022.2135032
[12] Z. S. Ahmed, M. RASHEED, H. S. Ahmed, Experimental and Theoretical NANOTECHNOLOGY, 10 (2026) 329. https://doi.org/10.56053/10.s.329
[13] A. Khaleefah, M. RASHEED, Experimental and Theoretical NANOTECHNOLOGY, 10 (2026) 289 https://doi.org/10.56053/10.s.289
[14] A. I. A. Ali, M. RASHEED, Experimental and Theoretical NANOTECHNOLOGY, 10 (2026) 277 https://doi.org/10.56053/10.s.277
[15] A. Raghdi, M. Heraiz, M. Rasheed, A. Keziz, Journal of the Indian Chemical Society, 101 (2024) 101413 https://doi.org/10.1016/j.jics.2024.101413
[16] S. S. Batros, M. Rasheed, H. K. Aity, A. A. Hatef, T. Saidani, Materials Chemistry and Physics, 355 (2026) 132243 https://doi.org/10.1016/j.matchemphys.2026.132243
[17] M. RASHEED, A. Khaleefah, Materials Chemistry and Physics, 353 (2026) 132112 https://doi.org/10.1016/j.matchemphys.2026.132112
[18] T. Saidani, S. Mokhtari, M. Rasheed, H. Lahmar, M. Trari, Journal of the Indian Chemical Society, 103 (2026) 102499 https://doi.org/10.1016/j.jics.2026.102499
[19] H. K. Aity, M. Rasheed, E. Dhahri, A. A. Hateef, T. Saidani, Journal of Materials Science, 61 (2026) 6226 https://doi.org/10.1007/s10853-026-12241-w
[20] Areej Adnan Hateef, Essebti Dhahri, M. Rasheed, Habiba Kadhim, Z. Abbas, N. Hassan, Physics and Chemistry of Solid State, 25 (2024) 801 https://doi.org/10.15330/pcss.25.4.801-810
[21] A.A. Salman, F.K. Mashee, A. Ramahi, I.M. Abdulameer, D.H.M., Exp. Theor. Nanotechnol. 9 (2025) 123 https://doi.org/10.56053/9.S.123
[22] A.K. Rahman, L.S. Chen, M.I. Al-Khalidi, Exp. Theo. NANOTECHNOLOGY 10 (2026) 115 https://doi.org/10.56053/10.1.109
[23] S.M. Kareem, J.T. Wallace, D.R. Singh, Exp. Theo. NANOTECHNOLOGY 10 (2026) 298 https://doi.org/10.56053/10.S.357